第 35 卷第 10 期
2019 年 10 月

无 机 化 学 学 报
CHINESE JOURNAL OF INORGANIC CHEMISTRY

Vol.35 No.10
1853-1860

由吡啶–三羧酸配体构筑的锌(Ⅱ)和锰(Ⅱ)配合物的合成、晶体结构、荧光及磁性质

黎 彧[1] 潘光敏[2] 邹训重[1] 冯安生[1] 游 逖*,[1] 邱文达*,[1]

([1]广东轻工职业技术学院,广东省特种建筑材料及其绿色制备工程技术研究中心/佛山市特种功能性建筑材料及其绿色制备技术工程中心,广州 510300)

([2]广东工业大学轻工化工学院,广州 510006)

摘要:采用水热方法,用吡啶–三羧酸配体(H_3L)和 2,2′-联咪唑(H_2biim 2,2′-biimidazole)、菲咯啉(phen)、2,2′-联吡啶(2,2′-bipy)分别与 $ZnCl_2$ 和 $MnCl_2·4H_2O$ 反应,合成了 1 个零维配合物$[Zn(H_2biim)_2(H_2O)_2][Zn(HL)(Hbiim)(H_2O)]_2·8H_2O$ (**1**)和 2 个具有一维链结构的配合物$[Mn(\mu\text{-}HL)(phen)(H_2O)]_n$ (**2**)、$\{[Mn(\mu\text{-}HL)(2,2'\text{-}bipy)(H_2O)]·0.5(2,2'\text{-}bipy)\}_n$ (**3**),并对其结构、荧光和磁性质进行了研究。结构分析结果表明 3 个配合物分别属于单斜晶系的 $P2_1/n$ 和 $P2_1/c$ 空间群。配合物 **1** 具有 3 个单核 Zn 单元组成的零维结构,这些单核单元通过 O–H…O/N 和 N–H…O 氢键作用进一步形成了三维超分子框架。配合物 **2** 和 **3** 具有一维链结构,而且这些链通过 O–H…O 氢键作用进一步形成了二维超分子网络。研究表明,配合物 **1** 在室温下能发出蓝色荧光,聚合物 **2** 中相邻 Mn(Ⅱ)离子间存在反铁磁相互作用。

关键词:配位聚合物;吡啶–三羧酸配体;荧光;磁性

中图分类号:O614.24+1;O614.71+1 **文献标识码**:A **文章编号**:1001-4861(2019)10-1853-08

DOI:10.11862/CJIC.2019.206

Syntheses, Crystal Structures, Luminescent and Magnetic Properties of One 0D Zinc(Ⅱ) and Two 1D Manganese(Ⅱ) Coordination Compounds Assembled from Pyridine-Tricarboxylate Blocks

LI Yu[1] PAN Guang-Min[2] ZOU Xun-Zhong[1] FENG An-Sheng[1] YOU Ao*,[1] QIU Wen-Da*,[1]

([1]*Guangdong Research Center for Special Building Materials and Its Green Preparation Technology / Foshan Research Center for Special Functional Building Materials and Its Green Preparation Technology, Guangdong Industry Polytechnic, Guangzhou* 510300, *China*)

([2]*School of Chemical Engineering and Light Industry, Guangdong University of Techlonogy, Guangzhou* 510006, *China*)

Abstract: One 0D zinic(Ⅱ) and two 1D manganese(Ⅱ) coordination compounds, namely $[Zn(H_2biim)_2(H_2O)_2][Zn(HL)(Hbiim)(H_2O)]_2·8H_2O$ (**1**), $[Mn(\mu\text{-}HL)(phen)(H_2O)]_n$ (**2**) and $\{[Mn(\mu\text{-}HL)(2,2'\text{-}bipy)(H_2O)]·0.5(2,2'\text{-}bipy)\}_n$ (**3**) have been constructed hydrothermally using H_3L (H_3L=4-(6-carboxy-pyridin-3-yl)-isophthalic acid), H_2biim (H_2biim= 2,2′-biimidazole), phen (phen=1,10-phenanthroline), 2,2′-bipy (2,2′-bipy=2,2′-bipyridine), and zinc or manganese chlorides. Single-crystal X-ray diffraction analyses reveal that three compounds crystallize in the monoclinic system, space groups $P2_1/n$ or $P2_1/c$. Compound **1** shows a 0D structure composed of three monomer Zn(Ⅱ) units, which is arranged into a 3D supramolecular framework through O–H … O/N or N–H … O hydrogen bonds.

收稿日期:2019-05-23。收修改稿日期:2019-06-14。

广东省高等职业院校珠江学者岗位计划资助项目(2015,2018),广东省自然科学基金(No.2016A030313761),广东轻院珠江学者人才类项目(No.RC2015-001),生物无机与合成化学教育部重点实验室开放基金(2016),广东省高校创新团队项目(No.2017GKCXTD001),广州市科技计划项目(No.201904010381),广东轻院科技成果培育项目(No.KJPY2018-010),广东轻院优秀青年基金(No.QN2018-007)和广东大学生科技创新培育专项(No.pdjh2019b0690)资助。

*通信联系人。E-mail:youao321@163.com,Qiuwdgq@hotmail.com

Compounds **2** and **3** feature a 1D metal-organic chain, which is assembled to a 2D supramolecular network through O–H⋯O hydrogen bond. The luminescent and magnetic properties for three compounds were also investigated. CCDC: 1917771, **1**; 1917772, **2**; 1917773, **3**.

Keywords: coordination polymer; pyridine-tricarboxylic acid; luminescent properties; magnetic properties

0 Introduction

Recently, construction of coordination polymers received considerable attention not only as a result of their intriguing varieties of molecular architectures and topologies but also for their applications in catalysis, magnetism, luminescence, and gas storage[1-5]. Although chemists and materials scientists have devoted much effort to rational design and syntheses coordination polymers, it is difficult to predict the structures of coordination polymers, because a lot of factors influence the construction of complexes, such as the structural features of organic ligands, the coordination requirements of metal ions, solvent systems, temperatures, and pH values[6-12].

In this regard, various types of aromatic polycarboxylic acids have been proved to be versatile and efficient candidates for constructing diverse coordination polymers due to their rich coordination chemistry, tunable degree of deprotonation, and ability to act as H-bond acceptors and donors[1,2,8,10,12-16].

As a combination of the aforementioned aspects and our previous research work, we have selected a novel pyridine-tricarboxylate ligand, 4-(6-carboxy-pyridin-3-yl)-isophthalic acid (H_3L, Scheme 1) and explored it for the construction of novel coordination polymers. The H_3L block possesses the following features: (1) it can twist and rotate freely to generate different angles between the phenyl-pyridine planes via the C-C bond to furnish a subtle conformational adaptation; (2) it has seven potential coordination sites (six carboxylate O donors and one N donor), which can lead to diverse coordination patterns and high dimensionalities, especially when acting as a multiply bridging spacer; (3) apart from a limited number of coordination compounds derived from H_3L[17-18], this acid block remains poorly used for the generation of coordination polymers. Given these features, the main objective of the present study consisted in the exploration of H_3L as a novel pyridine-tricarboxylate block for the assembly of diverse metal-organic networks.

Herein, we report the syntheses, crystal structures, luminescent and magnetic properties of Zn (Ⅱ) and Mn (Ⅱ) coordination compounds constructed from pyridine-tricarboxylate ligands.

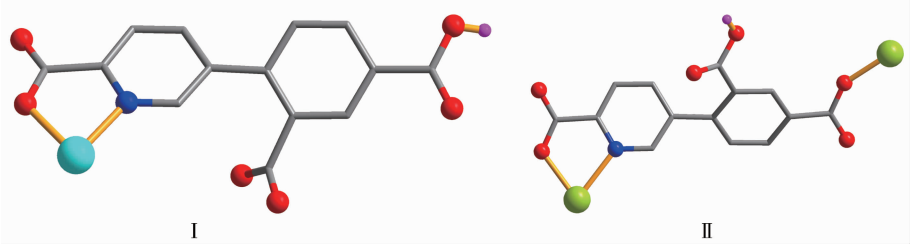

Ⅰ Ⅱ

Scheme 1 Coordination modes of HL^{2-} ligands in compounds 1 and 2

1 Experimental

1.1 Reagents and physical measurements

All chemicals and solvents were of AR grade and used without further purification. Carbon, hydrogen and nitrogen were determined using an Elementar Vario EL elemental analyzer. IR spectra were recorded using KBr pellets and a Bruker EQUINOX 55 spectrometer. Thermogravimetric analysis (TGA) data were collected on a LINSEIS STA PT1600 thermal analyzer with a heating rate of 10 ℃·min^{-1}. Excitation and emission spectra were recorded on an

Edinburgh FLS920 fluorescenc e spectrometer using the solid samples at room temperature. Magnetic susceptibility data were collected in the 2 ~300 K temperature range on a Quantum Design SQUID Magnetometer MPMS XL-7 with a field of 0.1 T. A correction was made for the diamagnetic contribution prior to data analysis.

1.2 Synthesis of $[Zn(H_2biim)_2(H_2O)_2][Zn(HL)(Hbiim)(H_2O)]_2\cdot 8H_2O$ (1)

A mixture of $ZnCl_2$ (0.027 g, 0.20 mmol), H_3L (0.057 g, 0.20 mmol), H_2biim (0.027 g, 0.20 mmol), NaOH (0.016 g, 0.40 mmol), and H_2O (10 mL) was stirred at room temperature for 15 min, and then sealed in a 25 mL Teflon-lined stainless steel vessel, and heated at 160 ℃ for 3 days, followed by cooling to room temperature at a rate of 10 ℃·h^{-1}. Colorless block-shaped crystals of **1** were isolated manually, and washed with distilled water. Yield: 44% (based on H_3L). Anal. Calcd. for $C_{52}H_{60}Zn_3N_{18}O_{24}$(%): C 41.16, H 3.99, N 16.62; Found(%): C 41.37, H 4.02, N 16.49. IR (KBr, cm^{-1}): 3 443w, 2 980w, 1 688m, 1 653s, 1 622 m, 1 602m, 1 577s, 1 485w, 1 455w, 1 419m, 1 368w, 1 311w, 1 245w, 1 169w, 1 122w, 1 046w, 1 016w, 944 w, 908w, 857w, 822w, 776w, 699w, 674w, 587w, 556w.

1.3 Synthesis of $[Mn(\mu\text{-}HL)(phen)(H_2O)]_n$ (2)

A mixture of $MnCl_2\cdot 4H_2O$ (0.040 g, 0.20 mmol), H_3L (0.057 g, 0.20 mmol), phen (0.040 g, 0.20 mmol), NaOH (0.016 g, 0.40 mmol), and H_2O (10 mL) was stirred at room temperature for 15 min, and then sealed in a 25 mL Teflon-lined stainless steel vessel, and heated at 160 ℃ for 3 days, followed by cooling to room temperature at a rate of 10 ℃·h^{-1}. Yellow block-shaped crystals of **2** were isolated manually, and washed with distilled water. Yield: 60% (based on H_3L). Anal. Calcd. for $C_{26}H_{17}MnN_3O_7$(%): C 58.00, H 3.18, N 7.81; Found(%): C 57.76, H 3.16, N 7.85. IR (KBr, cm^{-1}): 3 418w, 3 066w, 1 699m, 1 613s, 1 597s, 1 510w, 1 424 m, 1 383s, 1 296w, 1 245w, 1 163w, 1 143w, 1 087w, 1 041w, 1 005w, 929w, 898w, 847m, 817w, 776w, 724 w, 704w, 684w, 658w, 531w.

1.4 Synthesis of $\{[Mn(\mu\text{-}HL)(2,2'\text{-bipy})(H_2O)]\cdot 0.5(2,2'\text{-bipy})\}_n$ (3)

The preparation of **3** was similar to that of **2** except 2,2′-bipy was used instead of phen. After cooling the reaction mixture to room temperature, yellow block-shaped crystals of **3** were isolated manually, washed with distilled water, and dried. Yield: 40% (based on H_3L). Anal. Calcd. for $C_{29}H_{21}MnN_4O_7$(%): C, 58.79; H, 3.57; N, 9.46. Found(%): C, 58.91; H, 3.56; N, 9.52. IR (KBr, cm^{-1}): 3 427w, 3 060w, 1 702w, 1 607s, 1 544m, 1 471w, 1 439w, 1 382s, 1 298 w, 1 250w, 1 161w, 1 130w, 1 082w, 1 040w, 1 009w, 930w, 893w, 841w, 815w, 773m, 757w, 741w, 710w, 678w, 657w, 620w, 558w, 526w.

The compounds are insoluble in water and common organic solvents, such as methanol, ethanol, acetone and DMF.

1.5 Structure determination

Three single crystals with dimensions of 0.25 mm×0.23 mm×0.22 mm (**1**), 0.25 mm×0.22 mm×0.21 mm (**2**), and 0.27 mm×0.24 mm×0.23 mm (**3**) were collected at 293(2) K on a Bruker SMART APEX Ⅱ CCD diffractometer with Mo $K\alpha$ radiation (λ=0.071 073 nm). The structures were solved by direct methods and refined by full matrix least-square on F^2 using the SHELXTL-2014 program[19]. All non-hydrogen atoms were refined anisotropically. All the hydrogen atoms were positioned geometrically and refined using a riding model. In compound **3**, N atom of the lattice 2,2′-bipy is disordered over two sites, which are N4 and C27, with occupancy of 0.5. A summary of the crystallographic data and structure refinements for **1** and **2** is given in Table 1. The selected bond lengths and angles for compounds **1** and **2** are listed in Table 2. Hydrogen bond parameters of compounds **1** and **2** are given in Table 3 and 4.

CCDC: 1917771, **1**; 1917772, **2**; 1917773, **3**.

Table 1　Crystal data for compounds 1~3

Compound	1	2	3
Chemical formula	$C_{52}H_{60}Zn_3N_{18}O_{24}$	$C_{26}H_{17}MnN_3O_7$	$C_{29}H_{21}MnN_4O_7$
Formula weight	1 517.29	538.36	592.44

Continued Table 1

Crystal system	Monoclinic	Monoclinic	Monoclinic
Space group	$P2_1/n$	$P2_1/c$	$P2_1/c$
a / nm	1.072 9(2)	1.031 48(3)	1.033 19(3)
b / nm	1.155 27(17)	1.293 46(4)	1.375 68(5)
c / nm	2.506 3(3)	1.748 33(5)	1.764 49(5)
β / (°)	94.211(14)	90.874(3)	91.594(3)
V / nm^3	3.098 0(8)	2.332 33(13)	2.506 97(14)
Z	2	4	4
F(000)	1 560	1 100	1 216
θ range for data collection / (°)	3.469~25.048	3.359~25.049	3.338~25.047
Limiting indices	$-12 \leqslant h \leqslant 10$, $-13 \leqslant k \leqslant 11$, $-29 \leqslant l \leqslant 28$	$-12 \leqslant h \leqslant 8$, $-15 \leqslant k \leqslant 15$, $-20 \leqslant l \leqslant 18$	$-11 \leqslant h \leqslant 12$, $-16 \leqslant k \leqslant 11$, $-14 \leqslant l \leqslant 21$
Reflection collected, unique (R_{int})	10 998, 5 463 (0.128 9)	8 260, 4 126 (0.042 7)	8 368, 4 447 (0.041 1)
D_c / (g·cm^{-3})	1.627	1.533	1.570
μ / mm^{-1}	1.249	0.620	0.586
Data, restraint, parameter	5 463, 0, 439	4 126, 0, 343	4 447, 0, 370
Goodness-of-fit on F^2	1.022	1.025	1.041
Final R indices [$I \geqslant 2\sigma(I)$] R_1, wR_2	0.089 5, 0.114 2	0.046 2, 0.089 5	0.050 7, 0.090 9
R indices (all data) R_1, wR_2	0.220 3, 0.163 1	0.074 4, 0.108 8	0.080 3, 0.107 9
Largest diff. peak and hole / (e·nm^{-3})	463 and −461	273 and −269	374 and −394

Table 2 Selected bond distances (nm) and bond angles (°) for compounds 1~3

		1			
Zn(1)-O(1)	0.207 3(6)	Zn(1)-O(7)	0.206 0(6)	Zn(1)-N(1)	0.209 5(6)
Zn(1)-N(2)	0.221 1(8)	Zn(1)-N(3)	0.207 2(7)	Zn(2)-O(8)	0.243 2(7)
Zn(2)-O(8)A	0.243 2(7)	Zn(2)-N(6)	0.216 7(8)	Zn(2)-N(6)A	0.216 7(8)
Zn(2)-N(7)	0.200 7(8)	Zn(2)-N(7)A	0.200 7(8)		
O(7)-Zn(1)-N(3)	95.9(3)	O(7)-Zn(1)-O(1)	96.3(3)	O(1)-Zn(1)-N(3)	97.3(3)
O(7)-Zn(1)-N(1)	97.8(3)	N(3)-Zn(1)-N(1)	166.1(3)	O(1)-Zn(1)-N(1)	78.7(3)
O(7)-Zn(1)-N(2)	90.4(3)	N(3)-Zn(1)-N(2)	80.6(3)	O(1)-Zn(1)-N(2)	173.2(3)
N(1)-Zn(1)-N(2)	101.7(3)	N(6)-Zn(2)-N(7)	80.0(3)	N(6)A-Zn(2)-N(7)	100.0(3)
N(7)-Zn(2)-O(8)A	87.7(3)	N(7)-Zn(2)-O(8)	92.3(3)	N(6)-Zn(2)-O(8)A	92.6(3)
N(6)-Zn(2)-O(8)	87.4(3)				
		2			
Mn(1)-O(1)	0.207 3(2)	Mn(1)-O(5)A	0.217 6(2)	Mn(1)-O(7)	0.213 3(2)
Mn(1)-N(1)A	0.231 2(2)	Mn(1)-N(2)	0.229 8(3)	Mn(1)-N(3)	0.229 4(3)
O(1)-Mn(1)-O(7)	92.81(10)	O(1)-Mn(1)-O(5)A	104.57(9)	O(7)-Mn(1)-O(5)A	91.75(9)
O(1)-Mn(1)-N(3)	164.62(10)	N(3)-Mn(1)-O(7)	90.23(10)	O(5)A-Mn(1)-N(3)	90.39(9)
O(1)-Mn(1)-N(2)	92.31(10)	O(7)-Mn(1)-N(2)	108.11(9)	O(5)A-Mn(1)-N(2)	153.36(9)
N(3)-Mn(1)-N(2)	72.43(10)	O(1)-Mn(1)-N(1)A	88.87(9)	O(7)-Mn(1)-N(1)A	165.45(10)
O(5)A-Mn(1)-N(1)A	73.86(9)	N(3)-Mn(1)-N(1)A	91.97(9)	N(2)-Mn(1)-N(1)A	86.25(9)
		3			
Mn(1)-O(1)	0.209 0(3)	Mn(1)-O(6)A	0.218 1(2)	Mn(1)-O(7)	0.216 0(2)
Mn(1)-N(1)A	0.231 7(3)	Mn(1)-N(2)	0.227 1(3)	Mn(1)-N(3)	0.227 6(3)

Continued Table 2

O(1)-Mn(1)-O(7)	93.69(10)	O(1)-Mn(1)-O(6)A	99.41(10)	O(7)-Mn(1)-O(6)A	94.55(9)
O(1)-Mn(1)-N(2)	94.51(11)	N(2)-Mn(1)-O(7)	100.40(10)	O(6)A-Mn(1)-N(2)	158.85(11)
O(1)-Mn(1)-N(3)	166.07(11)	O(7)-Mn(1)-N(3)	86.57(10)	O(6)A-Mn(1)-N(3)	94.45(10)
N(3)-Mn(1)-N(2)	71.79(11)	O(1)-Mn(1)-N(1)A	88.63(10)	O(7)-Mn(1)-N(1)A	168.43(9)
O(6)A-Mn(1)-N(1)A	73.88(9)	N(2)-Mn(1)-N(1)A	90.71(10)	N(3)-Mn(1)-N(1)A	93.90(10)

Symmetry codes: A: $-x+1$, $-y+1$, $-z+2$ for **1**; A: $-x$, $y+1/2$, $-z+1/2$ for **2**; A: $-x+1$, $y-1/2$, $-z+1/2$ for **3**.

Table 3　Hydrogen bond parameters of compound 1

D–H…A	*d*(D-H) / nm	*d*(H…A) / nm	*d*(D…A) / nm	∠DHA / (°)
N(5)–H(2)…O(5)A	0.086	0.191 7	0.276 6	169.1
N(8)–H(8)…O(9)B	0.086	0.195 4	0.280 2	168.2
N(9)–H(9)…O(4)B	0.086	0.181 4	0.265 5	165.4
O(6)–H(6)…N(4)C	0.082	0.197 9	0.279 8	176.6
O(7)–H(1W)…O(9)	0.085	0.182 9	0.267 9	179.8
O(7)–H(2W)…O(11)D	0.085	0.177 1	0.262 1	179.3
O(8)–H(3W)…O(12)B	0.085	0.211 4	0.296 4	178.7
O(8)–H(4W)…O(5)E	0.085	0.199 8	0.284 8	179.5
O(9)–H(5W)…O(10)F	0.085	0.191 6	0.276 6	179.3
O(9)–H(6W)…O(4)	0.085	0.181 0	0.266 0	179.2
O(10)–H(7W)…O(6)G	0.085	0.200 5	0.285 5	179.9
O(10)–H(8W)…O(1)H	0.085	0.192 6	0.277 6	179.9
O(11)–H(9W)…O(3)I	0.085	0.191 1	0.276 1	179.2
O(12)–H(11W)…O(2)	0.085	0.208 0	0.293 0	179.6
O(12)–H(12W)…O(3)I	0.085	0.189 6	0.274 6	179.1

Symmetry codes: A: $x+1/2$, $-y-1/2$, $z+1/2$; B: $-x+1$, $-y+1$, $-z+1$; C: $x-1/2$, $-y-1/2$, $z-1/2$; D: $-x+3/2$, $y-1/2$, $-z+1/2$; E: $-x+1$, $-y$, $-z+1$; F: $-x+1/2$, $y-1/2$, $-z+1/2$; G: $x-1/2$, $-y+1/2$, $z+1/2$; H: $x-1$, y, z; I: x, $y+1$, z.

Table 4　Hydrogen bond parameters of compound 2

D–H…A	*d*(D-H) / nm	*d*(H…A) / nm	*d*(D…A) / nm	∠DHA / (°)
O(3)–H(3)…O(6)A	0.082	0.174 4	0.256 1	173.6
O(7)–H(1W)…O(2)B	0.091	0.173 0	0.263 1	171.3
O(7)–H(2W)…O(5)C	0.077	0.211 6	0.282 3	154.0

Symmetry codes: A: $-x-1$, $y+1/2$, $-z+1/2$; B: $-x+1$, $-y$, $-z$; C: $x+1$, $-y-1/2$, $z-1/2$.

Table 5　Hydrogen bond parameters of compound 3

D–H…A	*d*(D-H) / nm	*d*(H…A) / nm	*d*(D…A) / nm	∠DHA / (°)
O(3)–H(3)…O(5)A	0.082	0.174 8	0.255 5	169.5
O(7)–H(1W)…O(6)B	0.084	0.210 0	0.285 1	149.4
O(7)–H(2W)…O(2)C	0.082	0.185 7	0.265 9	165.3

Symmetry codes: A: $-x+2$, $y-1/2$, $-z+1/2$; B: $x-1$, $-y+3/2$, $z-1/2$; C: $-x$, $-y+1$, $-z$.

2　Results and discussion

2.1　Description of the structure

2.1.1　$[Zn(H_2biim)_2(H_2O)_2][Zn(HL)(Hbiim)(H_2O)]_2\cdot 8H_2O$ (**1**)

The structure of **1** is composed of a $[Zn(H_2biim)_2(H_2O)_2]^{2+}$ cation, two $[Zn(HL)(Hbiim)(H_2O)]^-$ anions, and eight lattice water molecules (Fig.1). In the cation, the Zn2 atom adopts an octahedral $\{ZnN_4O_2\}$ geometry filled by four N atoms from two H_2biim moieties and

two O atoms from two water ligands. In the anion, the Zn1 center is five-coordinated and reveals a quadrangular pyramidal $\{ZnN_3O_2\}$ environment, which is completed by one O and one N atom from the HL^{2-} block, two N donors from the H_2biim moiety, and one O atom from the water ligand. The lengths of the Zn-O and Zn-N bonds are 0.206 0(6)~0.243 2(7) nm and 0.200 7(8)~0.221 1(8) nm, respectively; these are within the normal values for related Zn(Ⅱ) derivatives[10,12]. In **1**, the HL^{2-} block acts as a terminal ligand (mode Ⅰ, Scheme 1). The dihedral angle of two aromatic rings in the HL^{2-} ligand is 30.54°. The cations and anions are multiply interconnected by the O–H⋯O/N or N–H⋯O hydrogen bonds to assemble a 3D H-bonded architecture (Fig.2 and Table 3).

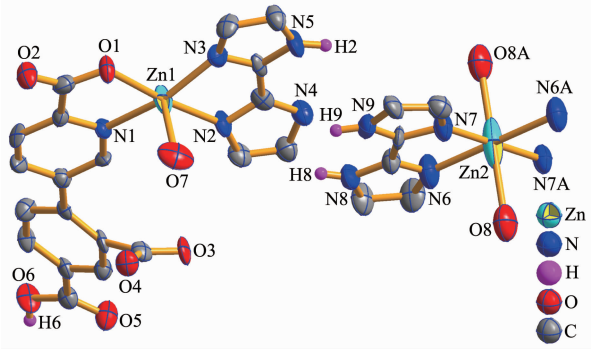

Lattice water molecules and H atoms except for those of the COOH group and H_2biim ligands are omitted for clarity; Symmetry code: A: $-x+1$, $-y+1$, $-z+2$

Fig.1 Drawing of the asymmetric unit of compound **1** with 50% probability thermal ellipsoids

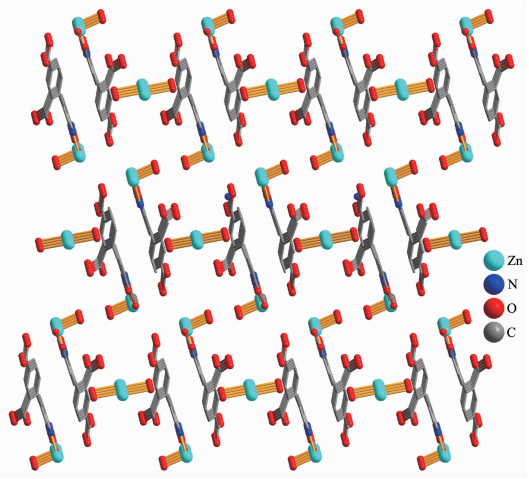

H_2biim ligands are omitted for clarity

Fig.2 View of a 3D H-bonded architecture in compound **1** along *b* axis

2.1.2 $[Mn(\mu\text{-HL})(phen)(H_2O)]_n$ (**2**) and $\{[Mn(\mu\text{-HL})(2,2'\text{-bipy})(H_2O)]\cdot 0.5(2,2'\text{-bipy})\}_n$ (**3**)

Compounds **2** and **3** feature essentially similar 1D chain structures (Table 1). A main difference concerns the type of supporting ligand: phen in **2** and 2,2′-bipy in **3**. Given similarity of structural and topological characteristics, the structure of **2** is described in detail as an example. The asymmetric unit of **2** bears one Mn1 center, one μ-HL^{2-} linker, one chelating phen and one terminal water ligand (Fig.3). The Mn1 center is six-coordinated and reveals a distorted octahedral $\{MnN_3O_3\}$ geometry. It is completed by two carboxylate O and one N donors from two μ-HL^{2-} moieties, a pair of phen N donors, and an H_2O ligand. The Mn-O (0.207 3(2)~0.217 6(2) nm) and Mn-N (0.229 4(3)~0.231 2(2) nm) bonds are within standard values[1,8,10]. The HL^{2-} block behaves as a tridentate μ-linker (Scheme 1, mode Ⅱ) that interconnects the adjacent Mn1 atoms to form a zigzag 1D metal-organic chain with a Mn1⋯Mn1 separation of 1.259 5(3) nm (Fig.4). Furthermore, such 1D chains

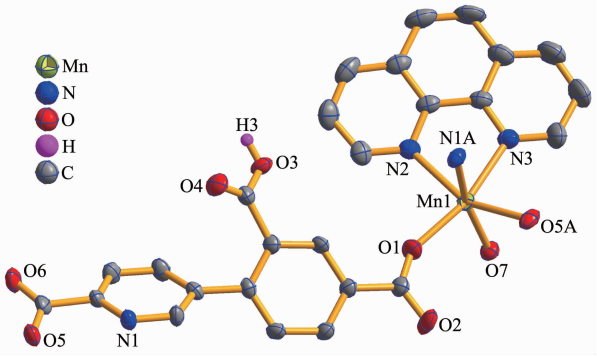

H atoms except for those of the COOH group are omitted for clarity; Symmetry code: A: $-x$, $y+1/2$, $-z+1/2$

Fig.3 Drawing of the asymmetric unit of compound **2** with 50% probability thermal ellipsoids

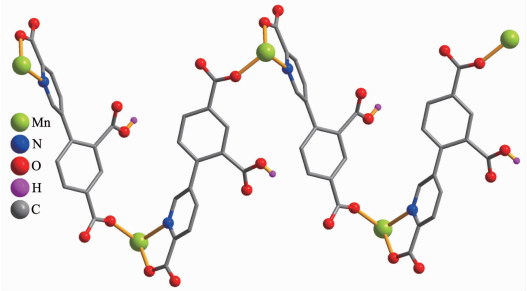

Phen ligands are omitted for clarity

Fig.4 View of 1D metal-organic chain along *c* axis

are further extended by H-bonds into a 2D H-bonded network (Fig.5 and Table 4).

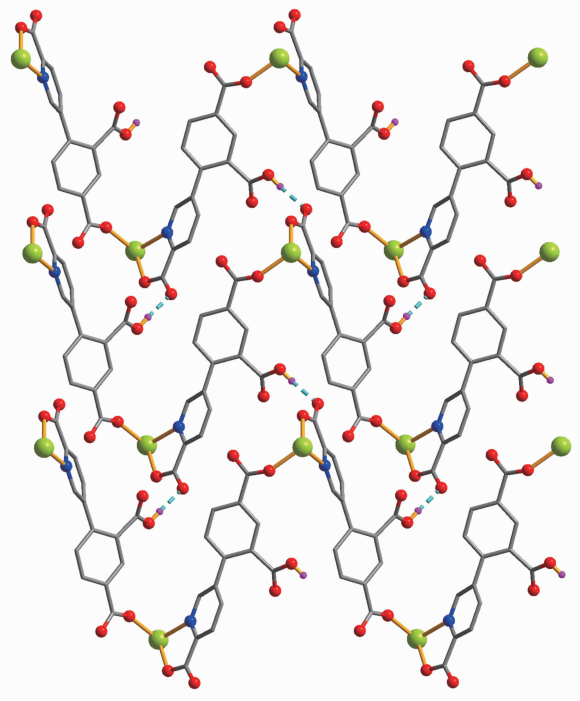

Phen ligands are omitted for clarity; Dashed lines present the H-bonds

Fig.5　Perspective of 2D supramolecular network parallel to *bc* plane in **2**

2.2　TGA analysis

To determine the thermal stability of compounds **1**~**3**, their thermal behaviors were investigated under nitrogen atmosphere by thermogravimetric analysis (TGA). As shown in Fig.6, TGA curve of compound **1** showed that there was a loss of eight lattice and four coordinated water molecules between 80 and 211 ℃ (Obsd. 14.1%, Calcd. 14.2%); further heating above 286 ℃ led to a decomposition of the dehydrated sample. Compound **2** lost its one water ligand in a range of 134~100 ℃ (Obsd. 3.3%, Calcd. 3.3%), followed by the decomposition at 356 ℃. For **3**, there is a thermal effect in the 140~227 ℃ range, corresponding to a removal of a half of one 2,2′-bipy moiety and the H_2O ligand (Obsd. 16.3%, Calcd. 16.2%); remaining samples are stable up to 290 ℃.

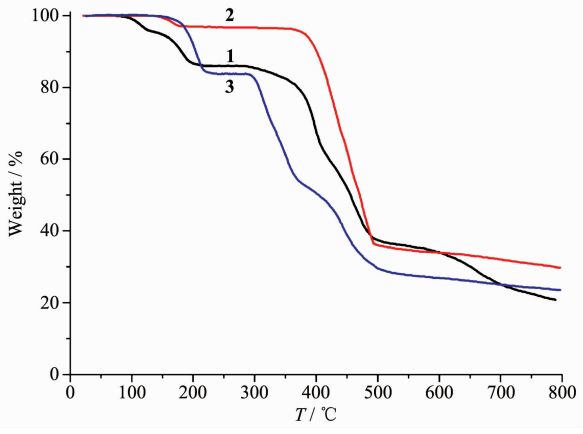

Fig.6　TGA curves of compounds **1**~**3**

2.3　Luminescent properties

Solid-state emission spectra of H_3L and zinc(Ⅱ) compound **1** were measured at room temperature (Fig. 7). The spectrum of H_3L revealed a weak emission with a maximum at 375 nm (λ_{ex}=322 nm). In comparison with H_3L, the coordination compound **1** exhibited more extensive emission with a maximum at 371 nm (λ_{ex}= 318 nm). These emissions correspond to intraligand π-π^* or n-π^* transition of H_3L[8,10,12]. Enhancement of the luminescence in **1** vs H_3L can be explained by the coordination of ligands to Zn(Ⅱ); the coordination can augment a rigidity of ligands and reduce an energy loss due to radiationless decay[1,10,12].

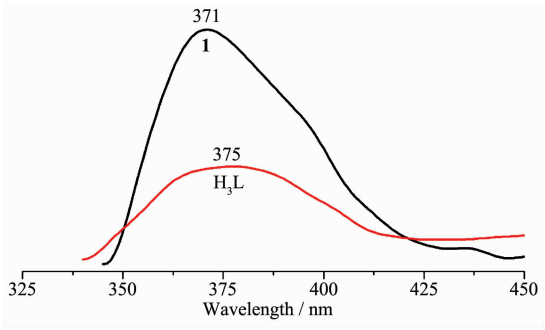

Fig.7　Solid-state emission spectra of H_3L and compound **1** at room temperature

2.4　Magnetic properties

Variable-temperature magnetic susceptibility measurements were performed on powder samples of **2** in a temperature range of 2~300 K (Fig.8). For the 1D Mn(Ⅱ) polymer **2**, the room temperature value of $\chi_M T$, 4.40 $cm^3 \cdot mol^{-1} \cdot K$, is close to the value (4.38 $cm^3 \cdot mol^{-1} \cdot K$) expected for a magnetically isolated high-spin Mn(Ⅱ) ion (S=5/2, g=2.0). If temperature was lowered, the $\chi_M T$ values decreased continuously to a minimum of 3.32 $cm^3 \cdot mol^{-1} \cdot K$ at 2.0 K. Between 2 and 300 K, the magnetic susceptibility could be fitted

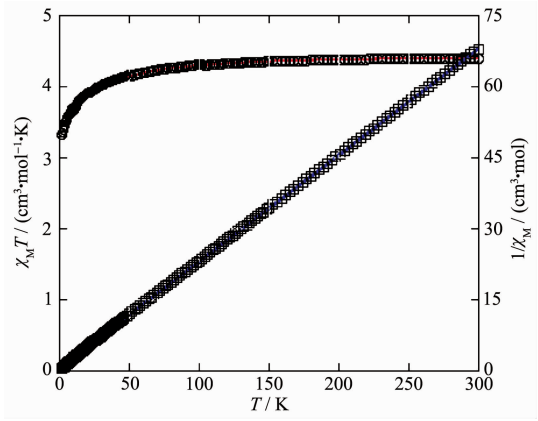

Red lines represent the best fit to the equations in the text; blue lines show the Curie-Weiss fitting

Fig.8 Temperature dependence of $\chi_M T$ (○) and $1/\chi_M$(□) for compound **2**

to the Curie-Weiss law with C=4.44 $cm^3 \cdot mol^{-1} \cdot K$ and θ=−2.73 K. These results also indicate an antiferromagnetic interaction between the adjacent Mn (Ⅱ) centers. We attempted to fit the data for **2** by applying the following expression for a 1D Mn(Ⅱ) chain[20]:

$$\chi_{chain}=[Ng^2\beta^2/(kT)](A+Bx^2)(1+Cx+Dx^3)^{-1}$$

with A=2.9167, B=208.04, C=15.543, D=2 707.2, and $x=|J|/(kT)$

Between 50 and 300 K, the susceptibility for **2** was simulated using this rough model, and resulting in J=−0.46 cm^{-1}, g=2.02, and R=2.17×10^{-5}. The negative J parameter indicates a weak antiferromagnetic exchange coupling between the adjacent Mn(Ⅱ) centers in **2**, which is in agreement with a negative θ value.

3 Conclusions

In summary, we have successfully synthesized and characterized three new zinc and manganese coordination compounds by using one pyridine-tricarboxylic acid as ligand under hydrothermal condition. Compound **1** shows a 0D structure composed of three monomers of Zn(Ⅱ) units. Compounds **2** and **3** feature 1D chains. Besides, the luminescent (for **1**) and magnetic (for **2**) properties were also investigated and discussed. The results show that such pyridine-tricarboxylic acid can be used as a versatile multifunctional building block toward the generation of new coordination polymers.

References:

[1] Gu J Z, Kirillov A M, Wu J, et al. *CrystEngComm*, **2013**,**15**: 10287-10303

[2] Gu J Z, Wen M, Cai Y, et al. *Inorg. Chem.*, **2019**,**58**:2403-2412

[3] Chen Q, Xue W, Lin J B, et al. *Chem. Eur. J.*, **2016**,**22**: 12088-12094

[4] Liu Z Q, Chen K, Zhao Y, et al. *Cryst. Growth Des.*, **2018**, **18**:1136-1146

[5] Hou L, Liu B, Jia L N, et al. *Cryst. Growth Des.*, **2013**,**13**: 701-707

[6] Pal S, Pal T K, Bharadwaj P K. *CrystEngComm*, **2016**,**18**: 1825-1831

[7] Zhang L N, Zhang C, Zhang B, et al. *CrystEngComm*, **2015**, **17**:2837-2846

[8] Gu J Z, Gao Z Q, Tang Y. *Cryst. Growth Des.*, **2012**,**12**:3312-3323

[9] Du M, Li C P, Liu C S, et al. *Coord. Chem. Soc.*, **2013**,**257**: 1282-1305

[10]Gu J Z, Cui Y H, Liang X X, et al. *Cryst. Growth Des.*, **2016**,**16**:4658-4670

[11]Wan J, Cai S L, Zhang K, et al. *CrystEngComm*, **2016**,**18**: 5164-5176

[12]Gu J Z, Cai Y, Qian Z Y, et al. *Dalton Trans.*, **2018**,**47**:7431-7444

[13]Peng Y W, Wu R J, Liu M, et al. *Cryst. Growth Des.*, **2019**, **19**:1322-1328

[14]GU Wen-Jun(顾文君), GU Jin-Zhong(顾金忠). *Chinese J. Inorg. Chem.*(无机化学学报), **2017**,**33**(2):227-236

[15]ZHAO Su-Qin(赵素琴), GU Jin-Zhong(顾金忠). *Chinese J. Inorg. Chem.*(无机化学学报), **2016**,**32**(9):1611-1618

[16]Gu J Z, Wen M, Liang X X. *Crystals*, **2018**,**8**:83

[17]Peng Y W, Wu R J, Liu M, et al. *Cryst. Growth Des.*, **2019**, **19**:1322-1328

[18]YOU Li-Xin(由立新), WANG Shu-Jü(王淑菊), XIONG Gang(熊刚), et al. *Chinese J. Inorg. Chem.*(无机化学学报), **2015**,**31**(2):323-328

[19]Spek A L. *Acta Crystallogr. Sect. C*: *Struct. Chem.*, **2015**, **C71**:9-18

[20]Fisher M E. *Am. J. Phys.*, **1964**,**32**:343-346